Powder Technology 312 (2017) 152–158

Contents lists available at ScienceDirect

Powder Technology

journal homepage: www.elsevier.com/locate/powtec

Rheological properties of gas and water atomized 17-4PH stainless steel MIM feedstocks: Effect of powder shape and size

Berenika Hausnerova [a,b,*], Bhimasena Nagaraj Mukund [a,c], Daniel Sanetrnik [a,b]

[a] Department of Production Engineering, Faculty of Technology, Tomas Bata University in Zlin, nam. T.G. Masaryka 5555, 760 01 Zlin, Czech Republic
[b] Centre of Polymer Systems, University Institute, Tomas Bata University in Zlin, Nad Ovcirnou 3685, 760 01 Zlin, Czech Republic
[c] Indo-US MIM Tec Pvt. Ltd., KIADB Industrial Area, Hoskote, Bangalore 562114, India

ARTICLE INFO

Article history:
Received 28 July 2016
Received in revised form 9 February 2017
Accepted 14 February 2017
Available online 21 February 2017

Keywords:
17-4PH gas atomized powder
17-4PH water atomized powder
Particle shape
Particle size
Viscosity
Torque
Critical solid loading

ABSTRACT

Influence of powder shape resulting from the fabrication route (gas or water atomization) together with the effect of mean particle size and solid loading on rheological properties of highly filled metal powder feedstocks was investigated as a key to processing of Metal Injection Molding (MIM) parts without voids and cracks. Eight 17-4PH gas or water atomized powders varying in the mean particle diameters from 3 to 20 μm were admixed into paraffin wax/high density polyethylene (50/50) binder at powder loadings up to 70 vol.%. The relative viscosity data obtained from capillary rheometer was fitted with rheological models to evaluate maximum loading along with the determination of the same parameter using time dependent torque measurement. It was found out that for coarse particles the processability in terms of rheological behavior is better in case of gas atomized powders in accordance with previous findings, but in case of fine powders, water atomized powders showed higher performance.

1. Introduction

Metal injection molding (MIM) offers more advantages in terms of manufacturing complicated profiles, lower cost and higher volume production than conventional machining. Starting from compounding and injection molding, and proceeding with debinding and finally sintering, MIM represents a multiple-step processing route. Mixing of metal powder and binder involves dispersion of metal powders in a polymer binder to form a highly filled compound called feedstock. During injection molding, feedstocks are injected into the die cavity at the required processing temperature and pressure to form so called green components with the desired shape. The green components are then debound to remove polymers, and finally sintered to nearly theoretical density [1].

The knowledge of the role of the individual powder characteristics (shape, size, particle size distribution) is essential to manufacture defect free MIM products. It has been generally accepted that gas atomized powder with spherical morphology can be packed to higher levels than irregularly shaped water atomized powders [1]. This aids higher sintered density in the products based on a gas atomized powder compared to a water atomized powder as previously shown e.g. for 316 L stainless steel [2], Ti64 [3] or 17-4PH [4], where water atomized powders were sintered up to 97% of the theoretical density compared to 99% achieved for gas atomized powders. The poor packing characteristics of water atomized powder along with the presence of oxides (which enhanced porosity and grain boundary) limited a complete densification. Mechanical tests performed in 17-4PH [4] indicate that the water atomized powder has lower mechanical performance than the gas atomized powder due to the higher porosity.

Along with higher packing density, spherical morphology of powders may also improve moldability and filling characteristics by reducing mixture viscosity during injection molding [1]. A regular, particularly plate–like shape, further improves the resistance to deformation as the particles tend to flow and orientate in the particle direction, but on the other hand evokes an anisotropic shrinkage during sintering [5]. Major disadvantage of using spherical powder morphology consists in a reduction of a component strength after binder removal in comparison to an irregular morphology of water atomized powders [6,7]. However, the shape retention can (to some extent) be compensated for gas atomized powders by decreasing the particle size of the powders enhancing thus the inter-particle contact per unit volume [1].

Generally, a MIM powder is recommended to have particle size ranging from 0.5 to 20 μm [1]. Packing of fine particles results in agglomeration due to strong cohesive forces affecting particle packing characteristics. Agglomeration tends to deteriorate mixing homogeneity, viscosity and stability of the feedstock. However, to some extent, an

* Corresponding author at: Department of Production Engineering, Faculty of Technology, Tomas Bata University in Zlin, nam. T.G. Masaryka 5555, 760 01 Zlin, Czech Republic.
E-mail address: hausnerova@ft.utb.cz (B. Hausnerova).

http://dx.doi.org/10.1016/j.powtec.2017.02.023

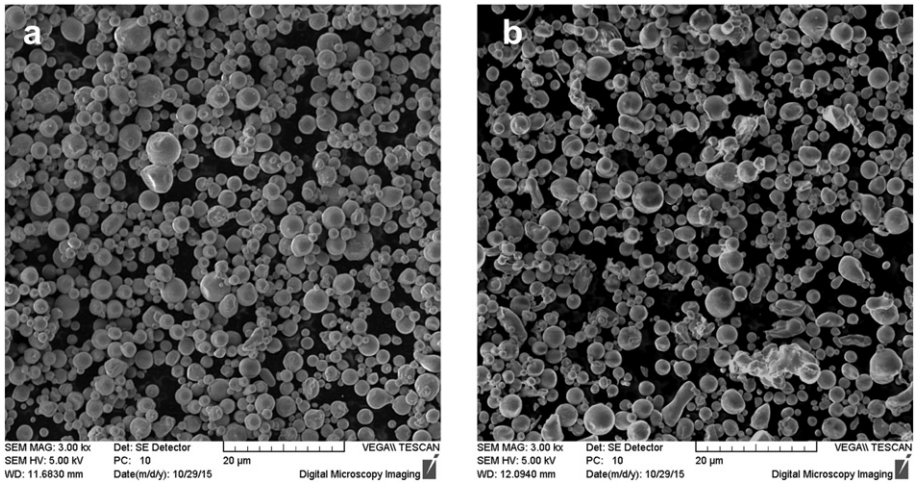

Fig. 1. SEM of the finest – about 3 μm mean diameter - 17-4PH gas (a) and water (b) atomized powders.

increase of mixing shear might reduce agglomerate size along with reduction in viscosity and improved stability of the feedstock. If finer and coarser powder particle sizes are compared, finer particles with enhanced tendency to form agglomerates result in lower packing density, higher mixing time - due to higher interparticle friction, higher mixture viscosity, and hence difficulty to inject into a cavity, higher compact strength, slow rate of binder removal - due to higher surface area of contact, but faster sintering and better shape retention [8].

An effective injection molding requires feedstocks with low viscosity, low activation energy and low flow behavior index. MIM compounds are sensitive to sudden changes in shear rate during molding of complicated profiles. At a certain shear rate, particles in a feedstock cannot form layers and slide over each other, and viscosity decrease along shear rate (shear thinning) may turn into the opposite trend (dilatant flow), especially for irregularly shaped particles [9,10]. At the same time, the systems filled close to their maximum packing fraction are subject to the separation of the binder from the solid phase (powder) [11–14].

Thus, the rheological analysis is crucial to optimize this MIM step. Further, homogeneity of feedstock or even assumptions on miscibility within binder components can be derived from the rheological data. In this paper, the rheology is employed to compare the feedstocks of various particle sizes produced either by gas or water atomization.

2. Experimental

2.1. Materials

Four different particle size distributions were chosen for each stainless steel 17-4PH gas and water atomized powders in the present study. Figs. 1 and 2 depict the morphology of finest and coarsest powders, respectively, evaluated with scanning electron microscope (SEM, VEGA II LMU, TESCAN). Pycnometer density and tap density of the individual powders, denoted in terms of their mean particle size, were determined according to MPIF 46 and the results are summarized in Table 1.

The complete particle size distribution of 17-4PH gas and water atomized powder was measured using laser scattering method (Microtrac S3500) and the results are summarized in Table 2. Particle size distribution slope parameter called S_w was determined from [1]

$$S_w = 2.56/\log(D_{90}/D_{10}) \quad (1)$$

This parameter is the slope of the log-normal cumulative distribution. Higher the value of S_w, the narrower particle distribution is. Narrow particle size distribution (S_w of 4–7) of powder will generally result in high viscosity of a feedstock, whereas broad particle size distribution (S_w of 2–4) means easy-to-mold low viscosity material [1].

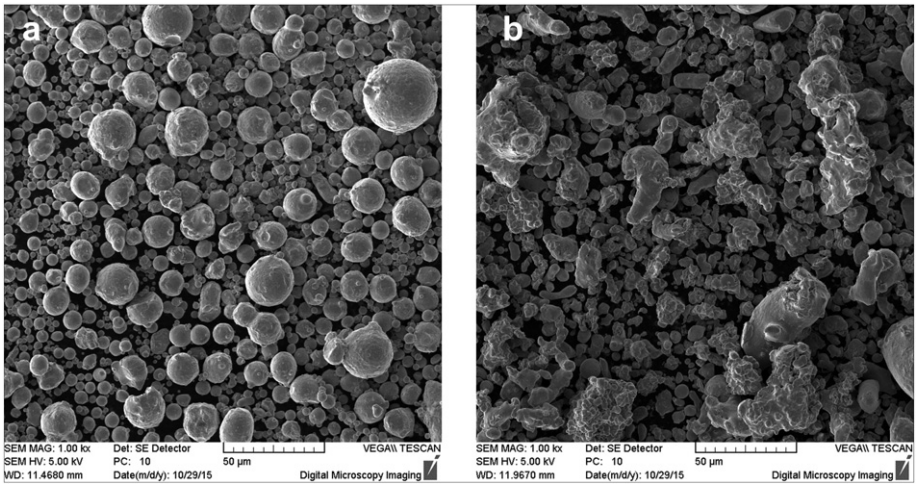

Fig. 2. SEM of the coarsest – about 20 μm mean diameter - 17-4PH gas (a) and water (b) atomized powders.

Table 1
Characteristics of 17-4PH gas and water atomized powders.

Mean particle size, D_{50} (μm)		Specific surface area (m^2/g)		Pycnometer density (g/cm^3)		Tap density (g/cm^3)	
Gas	Water	Gas	Water	Gas	Water	Gas	Water
3.3	3.3	0.53	0.40	7.80	7.71	4.1	3.9
8.0	6.5	0.31	0.36	7.78	7.68	4.3	4.2
11.1	10.1	0.23	0.34	7.85	7.66	4.6	4.2
20.0	19.3	0.15	0.22	7.88	7.71	4.8	4.1

Table 2
Particle size distribution (PSD) and PSD slope parameters of 17-4PH gas and water atomized powders.

Powder code		D_{10} (μm)		D_{50} (μm)		D_{90} (μm)		S_w	
Gas	Water	Gas	Water	Gas	Water	Gas	Water	Gas	Water
3	3	1.8	1.8	3.3	3.3	6.0	5.9	4.90	4.88
8	7	3.7	2.8	8.0	6.5	16.0	12.0	4.03	4.05
11	10	3.8	4.0	11.1	10.1	28.4	21.9	2.93	3.47
20	19	6.5	6.9	20.0	19.3	47.1	47.6	2.98	3.04

Binder composed of 50/50 mixture of paraffin wax (PW, Polyaid G101, Gujarath Waxes, density 0.91 $g \cdot cm^{-3}$, melting point 59 °C) and high density polyethylene (HDPE, H2105, Huntsman, density 0.96 $g \cdot cm^{-3}$, melting point 130 °C) as previously used for both metal (steel) and ceramic (alumina) based feedstocks [15–17].

2.2. Methods

Mixing of feedstocks at various solid loadings was performed using Haake PolyLab torque rheometer. It has a mixer capacity of 69 cm^3 with a mixing chamber divided into 3 segments and a temperature of each segment is monitored using in-built thermocouples. The 80% of this volume was used to mix the powder/binder mixtures at a temperature of 180 °C. When the blades started to rotate at 40 rpm, small amount of pre-mixed powder/binder compound was poured into the mixing chamber. Mixing time was fixed at 15 and 30 min for lower (10 and 30 vol.%) powder loadings and the feedstock compositions of 50 vol.% and higher, respectively.

Torque was recorded as a function of time at powder loading levels up to 70 vol.% before finding the critical filling level as a state, where a stable torque value, indicating homogenous mixing and/or uniform dispersion of a powder within a binder, turns into a fluctuating one. Close to the critical level, the powder concentration was raised in 1 vol.% steps only in order to evaluate the maximum loading precisely.

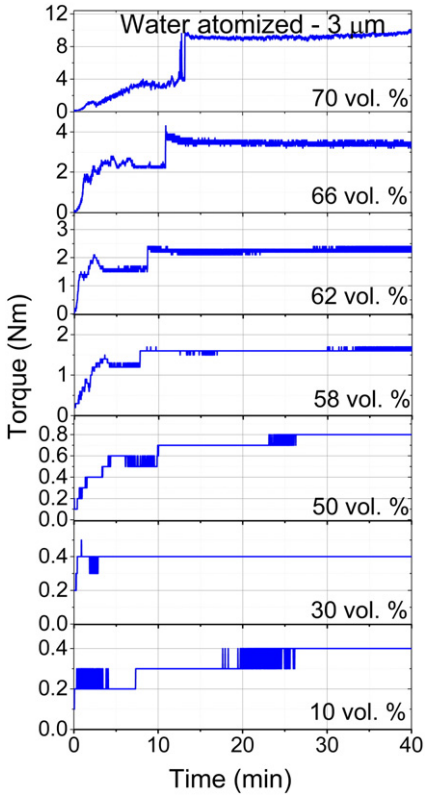

Fig. 4. Representative (3 μm water atomized feedstock) cause of torque development with time upon powder loading.

To study the flow behavior of the feedstocks, a single bore capillary rheometer (Instron, model SR 20) with a plane (180°) capillary entrance, diameter 1 mm and an L/D ratio of 20 was employed. The constant piston speed varied up to a maximum shear rate of 10^4 s^{-1}. The apparent shear rate was related to the volumetric flow rate, and the diameter of the capillary, while shear stress was related to the pressure drop in the capillary and its diameter/length ratio. The apparent viscosity is the ratio of apparent shear stress and apparent shear rate. The experimental temperature varied from 170 to 190 °C. Each data point was derived from three independent measurements.

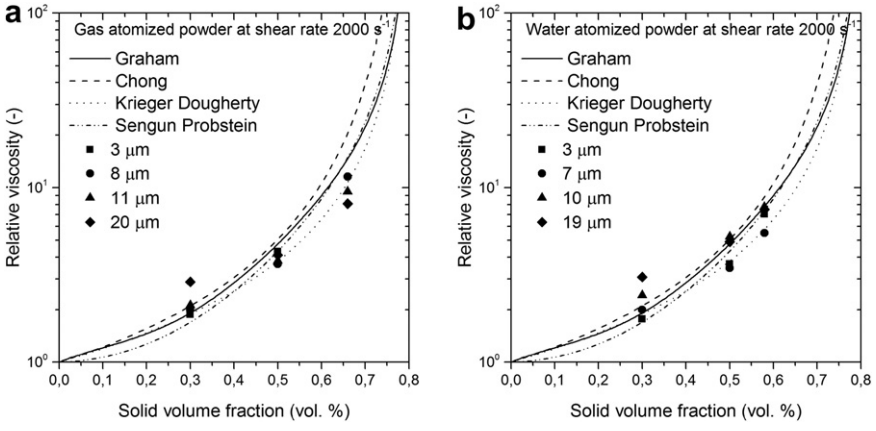

Fig. 3. Relative viscosity as a function of solid volume fraction data of 17-4PH gas (a) and water (b) atomized feedstocks fitted with the rheological models.

Table 3
Critical solid loading values of 17-4PH gas and water atomized feedstocks obtained from torque measurement.

Critical solid loading (vol.%)							
3 μm		8 μm		11 μm		20 μm	
Gas	Water	Gas	Water	Gas	Water	Gas	Water
67	68	66	70	70	66	70	66

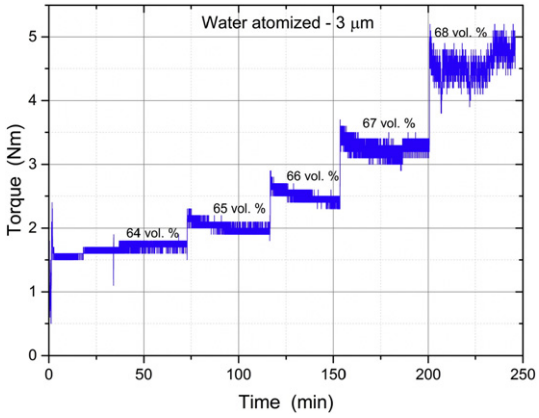

Fig. 5. Detailed torque analysis of the powder concentration region close to the critical solid loading – example for 3 μm water atomized feedstock.

3. Results and discussion

To understand the differences in rheological properties between gas and water atomized 17-4PH feedstocks, similar mean particle diameters of powders (D_{50}) as well as particle size distribution slope parameter (S_w) have been selected for the study (Table 2), where each powder is denoted by its mean particle diameter. S_w of each distribution was calculated to predict the suitability of the powder for injection molding; the obtained S_w values are also included in Table 2. The highest S_w of 4.90 and 4.88 observed for both gas and water atomized powders, respectively, belonged to mean particle size of 3 μm indicating narrow particle size distributions. On the other hand, the lowest S_w (2.98 and 3.04) were observed in the case of gas and water atomized powders of the mean particle size of about 20 μm, showing the broad particle size distributions of powder, which might be a general indication of an easy mixing of powders with lower surface area [1].

Nevertheless, such general statements often fail when the complex powder characteristic is considered, and thus, the rheological testing of the individual influences of the particle size (particle size distribution) and the shape of particles derived from a processing route is desirable in order to investigate the flow behavior of the feedstocks during mixing and molding.

First, an optimal loading derived from a critical (maximum) value can be obtained from rheological measurements. The rheological models containing a parameter of a critical solid loading (CSL) applied on the investigated gas and water atomized powder feedstocks were selected based on our previous review [18], where the applicability of various models on MIM compounds was examined. Critical solid loading

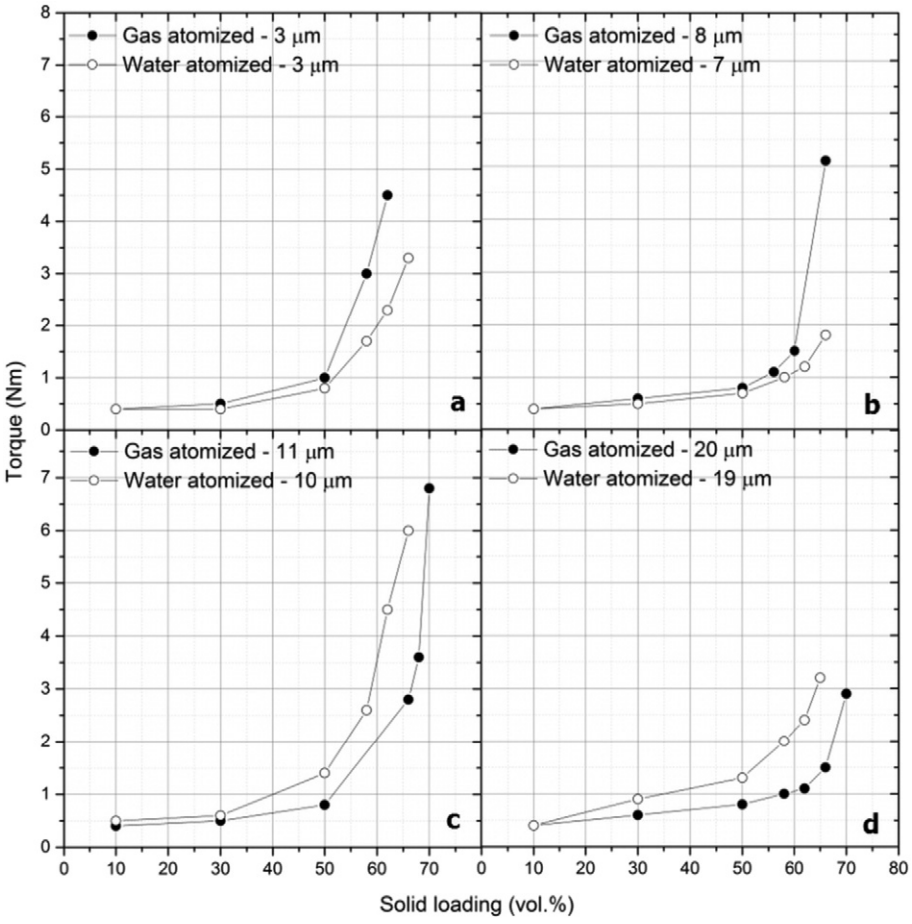

Fig. 6. Torque values obtained as a function of solid loading of gas and water atomized feedstocks based on: a) 3 μm, b) 7 and 8 μm, c) 11 and 10 μm, and d) 20 and 19 μm powders, respectively.

parameter ϕ_m was evaluated from the rheological models relating relative viscosity η_r to volume fraction of powder in a feedstock ϕ:

Graham's theoretical model [19]

$$\eta_r = \frac{9}{4}\left(1+\frac{H_0}{2a}\right)^{-1}\cdot\left[\frac{1}{(H_0/a)}-\frac{1}{(1+H_0/a)}-\frac{1}{\left(1+(H_0/a)^2\right)}\right] + (1+2.5\varphi) \quad (2)$$

where

$$\frac{H_0}{a} = 2\left[\left(\frac{\varphi_m}{\varphi}\right)^{1/3}-1\right] \quad (3)$$

Sengun-Probstein's semi-empirical model [20] calculating energy dissipation in a unit cell using the hydrodynamic lubrication concept for two spheres of equal sizes, approaching along their line of centre

$$\eta_r = 1 + C\left(\frac{3\pi}{8}\right)\left(\frac{\beta}{\beta+1}\right)\left[\frac{3+4.5\beta+\beta^2}{\beta+1}-3\left(\frac{\beta+1}{\beta}\right)\ln(\beta+1)\right] \quad (4)$$

where C is an undetermined proportionality constant, and β is a parameter related to the particle volume fraction in terms of the maximum packing fraction, such that the separation between the particle surfaces approaches zero in the limit $\phi \to \phi_m$.

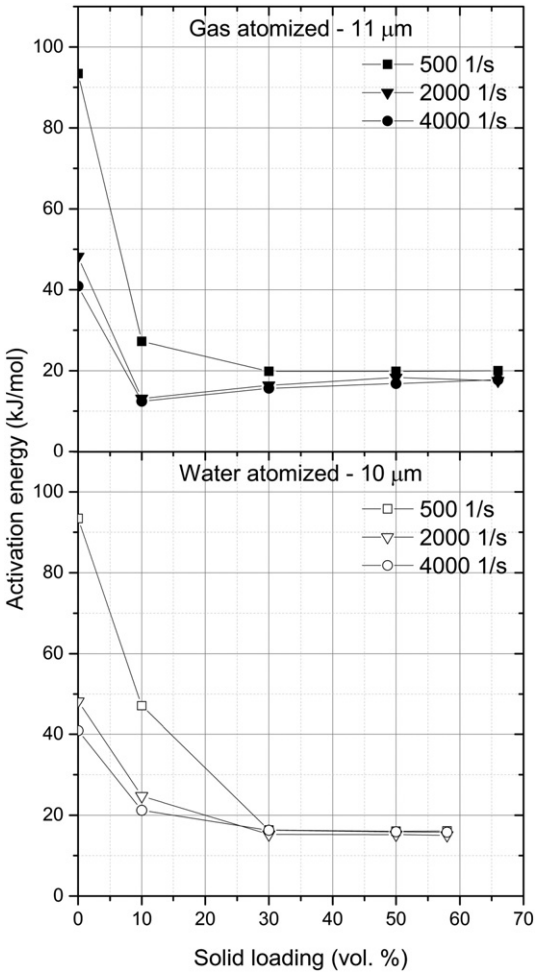

Fig. 7. Activation energy of representative gas (11 μm) and water (10 μm) atomized powder feedstocks derived at various constant shear rates as a function of solid loading.

The parameter is given by the relation

$$\beta = \frac{(\varphi/\varphi_m)^{1/3}}{1-(\varphi/\varphi_m)^{1/3}} \quad (5)$$

Chong et al. [21]

$$\eta_r = \left[1+0.75\left(\frac{\varphi/\varphi_m}{1-\varphi/\varphi_m}\right)\right]^2 \quad (6)$$

and Krieger Dougherty's semi-empirical relation [22]

$$\eta_r = \left(1-\frac{\varphi}{\varphi_m}\right)^{-k\varphi_m} \quad (7)$$

where k is a parameter found to be 2.5 for systems of rigid spheres.

These models were the only ones able to some extent fit the experimental data for a limited range of feedstocks concentration 10, 30 and 50 vol.% (Fig. 3), but they revealed rather unrealistic value of CSL 80 vol.%. Other models tested according to [18] failed completely. Therefore, the experimental evaluation of CSL, and following optimization of feedstocks loading from the torque measurement, has been preferred in this study.

It was carried out using measurement of the torque variation with time for solid loadings of 10, 30, and 50 vol.% for both types of powder, and additionally in the individual steps up to 70 vol.% for both gas and water atomized powders. The representative cause of torque is demonstrated in Fig. 4 for the smallest 3 μm water atomized powder based compound. Fluctuations/variations in torque observed for higher loading indicated the proximity of the critical solid loading (CSL) as the binder becomes locked in the interparticle space offering more resistivity to the flow. CLS parameters summarized in Table 3 were evaluated precisely from the detailed torque evaluation by 1 vol.% powder added step by step within the critical region as can been seen from the example analysis in Fig. 5.

From Table 3 it becomes evident that general statement concerning the advantage of spherical vs. irregular shape in terms of higher packing applies only for coarser particles (mean particle sizes about 11 and 20 μm), where the higher CSL is obtained for gas atomizes powders. The opposite (although not pronounced) trend was obtained for 3 and 8 μm fine powders, where slightly higher CSL is obtained for water atomized powders in comparison to feedstocks based on gas atomized

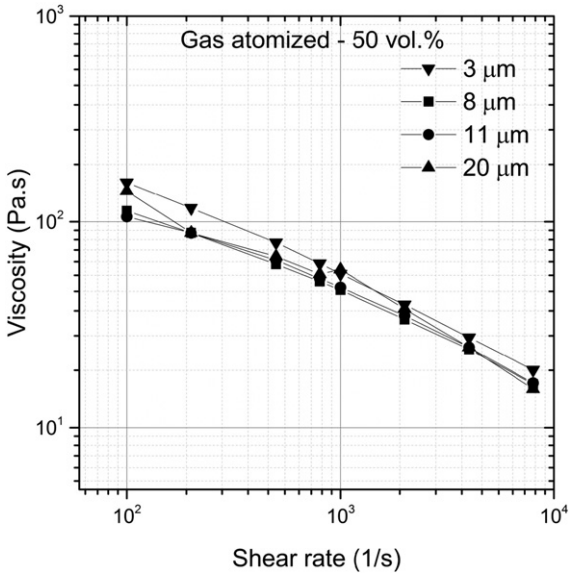

Fig. 8. Viscosity as a function of shear rate for 50 vol.% of gas atomized feedstocks.

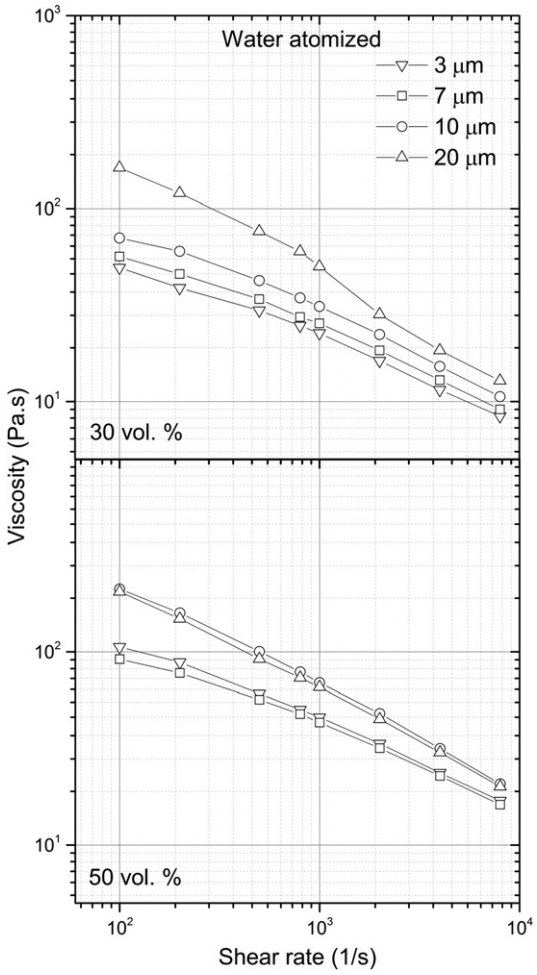

Fig. 9. Viscosity as a function of shear rate for 30 and 50 vol.% of water atomized feedstocks.

powders. Thus, in the case of fine powders, the influence of the size seems to overcome that of the shape as the water atomized powders show higher CSL.

Further, Fig. 6 demonstrates the torque values of both gas and water atomized feedstocks obtained at various solid loading. At lower solid loading (up to 30 vol.%), the increase in torque value is marginal, whereas, due to the higher friction between the powder particles at higher solid loading (which supports the previous experimental work reported in [8]), the increase in torque value is considerable. If water and gas atomized powders are compared, the importance of particle sizes is evident again. For the smaller mean diameter powders (3 and 8 μm) the torques of gas atomized powder are higher than those for water atomized ones, while for coarser ones (11 and 20 μm), the trend is opposite. It can be attributed to the irregular morphology of the water atomized powders, which generate higher friction [1] compared to the gas atomized powders.

Further, specific surface area of all the chosen powders was measured to understand the processability of the powders when mixed with binders. It can be noted that specific area increases with reduction in particle size of the powders as it represents the indirect measure of average particle diameter [1]. Highest specific surface areas of 0.53 m^2/g and 0.40 m^2/g were observed for 3 μm gas and water atomized powders, respectively, which indicates that the powder needs more binder to wet the powder particles, and consequently will flow with the higher resistance to shear deformation (higher viscosity), e.g. in [23]. At the same time, the powders with higher surface area can be sintered almost near to their theoretical density as the surface area is related to surface energy driving sintering [1]. The surface area of gas atomized powder of 3 μm powder is higher than that of 3 μm water atomized powder, whereas the trend is clearly opposite for the coarse particles studied (11 and 20 μm).

Both gas and water atomized powder feedstocks exhibited pseudoplastic behavior with decrease in viscosity with an increase of shear rate. Temperature sensitivity of the feedstocks can be derived from the cause of activation energy as a function of solid loading upon various shear conditions. From the example given in Fig. 7 it is evident that the sensitivity to temperature is very similar for both gas and water atomized powders. This applies for all studied compounds.

For gas atomized powders, the viscosity increases with the decreasing of the particle size as expected, however, overall differences are rather small (Fig. 8). On the other hand, in case of water atomized powder, the trend is quite opposite and well pronounced, as can be seen from the example of 30 and 50 vol.% (Fig. 9), where coarser particles are more resistant to flow than the smaller particles. It means that for the set of MIM compounds investigated, generally accepted presumption of better flowability derived from viscosity causes of larger particles fails for irregularly shaped water atomized feedstocks.

Finally, the viscosity cause of both gas and water atomized feedstocks show some flow fluctuations in shear stress (pressure drop) at low concentrations as clearly visible on the example of water atomized powders, where the effect is more pronounced (Fig. 10). For highly filled polymeric systems as MIM feedstocks, Isayev and Fan [24] observed unstable flow for polypropylene filled up to 65 vol.% by silicon powder. In their case the unstable flow occurred on capillary rheometer over the entire range of shear rates studied (10^0–10^2 s^{-1}). On the other hand, Yilmazer et al. [25] proposed a different area of unstable flow when investigated suspensions of poly(butadiene acrylonitrile acrylic acid) with 73 vol.% of ammonium sulphate powders (particle sizes 400 μm and 23 μm). They found that for such compounds steady flows could not be obtained under a critical shear stress. The mechanism of instabilities lies in a separation of binders out of compounds [25–27].

Yilmazer et al. [25] also pointed out that the stable flow could not be obtained for the compound containing greater particles (400 μm) whereas the smaller particles (23 μm) yielded stable flow. This finding is in accordance with our observations, where the fluctuations were most pronounced for the largest particles studied. However, according

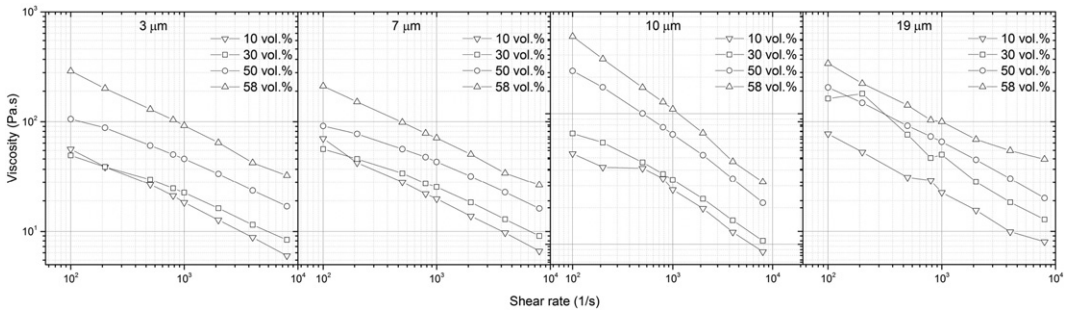

Fig. 10. Viscosity as a function of shear rate of water atomized feedstocks for powder sizes varying from 3 to 19 μm and powder concentrations up to 58 vol.%.

to their appearance, the instabilities detected for the investigated compounds cannot be attributed to the in-homogeneities within the feedstock arising from an insufficient mixing or a separation of feedstock components typical for highly concentrated compounds. Instead, the origin of these fluctuations is accounted to a spurt phenomenon, a typical flow instability occurring during flow of high-density polyethylene, which was employed as a polymer binder component [e.g. in 28]. As it can be seen from Fig. 10, the increasing powder loading has a stabilizing effect on the flow stability, because powder particles prevent polymer chain disentanglement on the channel wall.

4. Conclusion

The size as well as the shape of powder particles derived from the route of the powder manufacturing has a considerable effect on the processability of feedstocks based on 17-4PH stainless steel powders and paraffin wax/high density polyethylene (50/50) binder. It was found out that for coarse (11 and 20 μm) particles studied, the processability in terms of critical solid loading, viscosity and mixing torque values is more suitable in the case of gas atomized powders, whereas in the case of fine powders (3 and 8 μm), water atomized feedstocks show a better performance. The latter is rather opposite to generally accepted statements concerning the effect of particle shape on flow behavior of filled polymer melts. For the set of the investigated feedstocks, it seems that in the case of fine powders, the influence of size exceeds that of shape.

Acknowledgment

This work was supported by the Ministry of Education, Youth and Sports of the Czech Republic – Program NPU I (LO1504).

References

[1] R.M. German, A. Bose, Injection Molding of Metals and Ceramics, second ed MPIF - Metal Powder Industries Federation, Princeton, New Jersey, 1997.
[2] R.P. Koseski, P. Suri, N.B. Earhardt, R.M. German, Microstructure evaluation of injection molded gas and water atomized 316 stainless steel powder during sintering, Mater. Sci. Eng. A 390 (2005) 171–177.
[3] H.O. Gulsoy, N. Gulsoy, R. Calisici, Particle morphology influence on mechanical and biocompatibility properties of injection molded Ti alloy powder, Bio-Med. Mater. Eng. 24 (2014) 1861–1873.
[4] H.O. Gulsoy, S. Ozbek, T. Baykara, Microstructure and mechanical properties of injection molded gas and water atomized 17-4 PH stainless steel powder, Powder Metall. 50 (2007) 120–126.
[5] A. Mannschatz, A. Muller, T. Moritz, Influence of powder morphology on properties of ceramic injection moulding feedstocks, J. Eur. Ceram. Soc. 31 (2011) 2551–2558.
[6] D.F. Heany, R. Zauner, C. Binet, K. Cowan, J. Piemme, Variability of powder characteristics and their effect on dimensional variability of powder injection molded components, Powder Metall. 47 (2004) 144–149.
[7] S. Park, Y. Wu, D.F. Heaney, X. Zou, G. Gai, R.M. German, Rheological and thermal debinding behaviors in titanium powder injection molding, Metall. Mater. Trans. A 40A (2009) 215–222.
[8] B. Hausnerova, T. Kitano, I. Kuritka, J. Prindis, L. Marcanikova, The role of powder particle size distribution in processability of powder injection molding compounds, Int. J. Polym. Anal. Charact. 16 (2011) 141–151.
[9] R.L. Hoffman, Discontinuous and dilatant viscosity behaviour in concentrated suspensions. I. Observations of a flow instability, Trans. Soc. Rheol. 16 (1972) 155–173.
[10] B. Hausnerova, L. Marcanikova, P. Filip, P. Saha, Optimization of powder injection molding of feedstock based on aluminium oxide and multicomponent water-soluble polymer binder, Polym. Eng. Sci. 119 (2011) 2925–2932.
[11] P. Yaras, D.M. Kalyon, U. Yilmazer, Flow instabilities in capillary flow of concentrated suspensions, Rheol. Acta 33 (1994) 48–59.
[12] B. Hausnerova, Powder injection moulding - an alternative processing method for automotive items, in: M. Chiaberge (Ed.), Trends and Developments in Automotive Engineering, first ed.InTech, Vienna 2010, pp. 129–146.
[13] M. Jenni, L. Schimmer, R. Zauner, J. Stampfl, J. Morris, Quantitative study of powder binder separation of feedstocks, PIM Int. 2 (2008) 50–55.
[14] B. Hausnerova, D. Sanetrnik, P. Ponizil, Surface structure analysis of injection molded highly filled polymer melts, Polym. Compos. 34 (2013) 1553–1558.
[15] M.E. Sotomayor, A. Varez, B. Levenfoeld, Influence of powder particle size distribution on rheological properties of 316L powder injection molding feedstock, Powder Technol. 200 (2010) 30–36.
[16] G. Herranz, B. Levenfeld, A. Varez, J.M. Torralba, Development of new feedstock formulation based on high density polyethylene for MIM of M2 high speed steels, Powder Metall. 48 (2005) 134–138.
[17] P. Thomas-Veilma, A. Cervera, B. Levenfeld, A. Varez, Production of alumina parts by powder injection molding with a binder system based on high density polyethylene, J. Eur. Ceram. Soc. 28 (2008) 763–771.
[18] T. Honek, B. Hausnerova, P. Saha, Relative viscosity models and their application to capillary flow data of highly filled hard-metal carbide powder compounds, Polym. Compos. 26 (2005) 29–36.
[19] A.L. Graham, On the viscosity of suspensions of solid spheres, Appl. Sci. Res. 37 (1981) 275–286.
[20] M.Z. Sengun, R.F. Probstein, High-shear-limit viscosity and the maximum packing fraction in concentrated monomodal suspensions, Physicochem. Hydrodyn. 11 (1989) 229–241.
[21] J.S. Chong, E.B. Christiansen, A.D. Baer, Rheology of concentrated suspensions, J. Appl. Polym. Sci. 15 (1971) 2007–2021.
[22] I.M. Krieger, T.J. Dougherty, A mechanism for non-Newtonian flow in suspensions of rigid spheres, Trans. Soc. Rheol. 3 (1959) 137–152.
[23] A.V. Shenoy, Rheology of Filled Polymer Systems, first ed. Kluwer Academic Publishers, Dordrecht, 1999.
[24] A.I. Isayev, X. Fan, Steady and oscillatory flows of silicon-polypropylene ceramic compounds, J. Mater. Sci. 29 (1994) 2931–2938.
[25] U. Yilmazer, C.G. Gogos, D.M. Kalyon, Mat formation and unstable flow of highly filled suspensions in capillaries and continuous processors, Polym. Compos. 10 (1989) 242–248.
[26] B. Hausnerova, P. Saha, J. Kubat, Capillary flow of hard-metal carbide powder compounds, Int. Polym. Process. 14 (1999) 254–260.
[27] T. Honek, B. Hausnerova, P. Saha, Temperature dependent flow properties of powder injection molding compounds, Appl. Rheol. 12 (2002) 72–80.
[28] J.M. Piau, N. El Kissi, F. Toussaint, A. Mezghani, Distortions of polymer melts extrudates and their elimination using slippery surfaces, Rheol. Acta 34 (1995) 40–57.